Arnold Mathematical Journal (2023) 9:41–68
https://doi.org/10.1007/s40598-021-00195-7

RESEARCH CONTRIBUTION

A Symplectic Dynamics Proof of the Degree–Genus Formula

Peter Albers[1] · **Hansjörg Geiges**[2] · **Kai Zehmisch**[3,4]

Received: 15 September 2021 / Accepted: 26 November 2021 / Published online: 20 December 2021
© The Author(s) 2021

Abstract
We classify global surfaces of section for the Reeb flow of the standard contact form on the 3-sphere (defining the Hopf fibration), with boundaries oriented positively by the flow. As an application, we prove the degree-genus formula for complex projective curves, using an elementary degeneration process inspired by the language of holomorphic buildings in symplectic field theory.

Mathematics Subject Classification 37J05 · 14H50 · 32Q65 · 53D35

1 Introduction

A *global surface of section* for the flow of a non-singular vector field X on a three-manifold M is an embedded compact surface $\Sigma \subset M$ such that

(i) the boundary $\partial\Sigma$ is a union of orbits;

This work is partially supported by the Deutsche Forschungsgemeinschaft (DFG) through the SFB/TRR 191 'Symplectic Structures in Geometry, Algebra and Dynamics' (Project-ID 281071066 – TRR 191) and through the Heidelberg STRUCTURES Excellence Cluster under Germany's Excellence Strategy (EXC-2181/1 – 390900948).

✉ Hansjörg Geiges
geiges@math.uni-koeln.de

Peter Albers
palbers@mathi.uni-heidelberg.de

Kai Zehmisch
kai.zehmisch@rub.de

1 Mathematisches Institut, Universität Heidelberg, Im Neuenheimer Feld 205, 69120 Heidelberg, Germany

2 Mathematisches Institut, Universität zu Köln, Weyertal 86-90, 50931 Cologne, Germany

3 Mathematisches Institut, Justus-Liebig-Universität Gießen, Arndtstraße 2, 35392 Giessen, Germany

4 Present Address: Fakultät für Mathematik, Ruhr-Universität Bochum, Universitätsstraße 150, 44780 Bochum, Germany

(ii) the interior $\mathrm{Int}(\Sigma)$ is transverse to X;
(iii) the orbit of X through any point in $M \backslash \partial\Sigma$ intersects $\mathrm{Int}(\Sigma)$ in forward and backward time.

If one can find such a global surface of section, understanding the dynamics of X essentially reduces to studying the Poincaré return map $\mathrm{Int}(\Sigma) \to \mathrm{Int}(\Sigma)$, which sends each point $p \in \mathrm{Int}(\Sigma)$ to the first intersection point of the X-orbit through p with $\mathrm{Int}(\Sigma)$ in forward time.

In symplectic dynamics, where X is a Hamiltonian or Reeb vector field, there are a number of results on the existence or non-existence of global surfaces of section, e.g. [11–15,19]. Conversely, one can ask for the existence of flows with a given surface of section and return map. For instance, in [2] we describe a construction of Reeb flows on the 3-sphere S^3 with a disc-like global surface of section, where the return map is a pseudorotation; see also [1,16].

For Reeb flows on the 3-sphere coming from contact forms that define the standard tight contact structure, the following are the main facts known about the existence of global surfaces of section. Hofer, Wysocki and Zehnder [11, Theorem 1.3] give a sufficient criterion (dynamical convexity) for the existence of a disc-like global surface of section. Hryniewicz and Salomão [14, Theorem 1.3] describe a necessary and sufficient condition for a periodic Reeb orbit of a non-degenerate contact form to bound a disc-like global surface of section. A Reeb flow without a disc-like global surface of section has been constructed by van Koert [19]. It is not known if there is a Reeb flow (in the described class) without any global surface of section.

This motivates the question whether one can give a complete classification of global surfaces of section for a given flow. In the present paper, we consider the Hopf flow on the 3-sphere $S^3 \subset \mathbb{C}^2$, that is, the flow

$$\Psi_t : \ (z_1, z_2) \longmapsto (\mathrm{e}^{\mathrm{i}t} z_1, \mathrm{e}^{\mathrm{i}t} z_2), \quad t \in \mathbb{R}, \tag{1}$$

defining the Hopf fibration $S^3 \to S^2$, as well as the induced flows on the lens space quotients $L(d, 1)$ of S^3. Our first main result, which is purely topological, gives a classification, up to isotopy, of the surfaces that can arise as global surfaces of section for these flows.

The second main result is a symplectic dynamics proof of the classical degree-genus formula for complex projective curves. This formula says that a non-singular complex algebraic curve of degree d in the projective plane $\mathbb{C}\mathrm{P}^2$ is topologically a connected, closed, oriented surface of genus

$$g = \frac{1}{2}(d-1)(d-2). \tag{2}$$

Our proof uses degenerations of complex projective curves in the spirit of Symplectic Field Theory (SFT). Perhaps surprisingly, the SFT point of view elucidates why (2) should be read as a sum $\sum_{k=1}^{d-2} k$. For a given non-singular complex projective curve of degree d, we describe a 1-dimensional family of curves starting at the given one and converging to a holomorphic building of height d in the sense of [3]. Each level in this holomorphic building has genus 0, and the gluing of level $k+2$ to level $k+1$

contributes k to the genus, $k = 1, \ldots, d-2$ (see Fig. 11). This may be regarded as a motivating example for the degenerations studied in SFT. We ought to point out that we do not use any actual results from SFT.

The 'standard' proof of the degree-genus formula, using branched coverings and the Riemann–Hurwitz formula, can be found in [18, Chapter 4]; see also [20, §21] and [8, p. 219].

Here is an outline of the paper. In Sect. 2 we construct some examples of surfaces of section for the Hopf flow. We show how certain equivalences between Seifert invariants can be interpreted as modifications of such surfaces.

In Sect. 3 we relate global surfaces of section for the Hopf flow on S^3 to those for the induced flow (which likewise defines an S^1-fibration) on the lens space quotients $L(d, 1)$. We then classify 1-sections in $L(d, 1)$, i.e. global surfaces of section that intersect each fibre exactly once. The classification of d-sections (Definition 2.1) for the Hopf flow on S^3 with all boundary orbits traversed positively is achieved in Sect. 4.

In Sect. 5 we discuss a number of examples how algebraic curves in $\mathbb{C}\mathrm{P}^2$ give rise to global surfaces of section for the Hopf flow. This allows one to determine the genus of these particular curves.

Finally, in Sect. 6 we prove the degree-genus formula, using genericity properties of algebraic curves. We give one proof directly from the classification of global surfaces of section for the Hopf flow. The second, more instructive proof, uses SFT type degenerations to interpret the degree-genus formula as as a sum $\sum_{k=1}^{d-2} k$. Technical details of the SFT type convergence are relegated to Sect. 7.

2 The Hopf Flow

Our aim is to describe surfaces of section for the Hopf flow (1) on the 3-sphere S^3. Thinking of S^3 as the unit sphere in $\mathbb{R}^4$, we can define a 1-form α_{st} on S^3 by

$$\alpha_{\mathrm{st}} = \big(x_1\,\mathrm{d}y_1 - y_1\,\mathrm{d}x_1 + x_2\,\mathrm{d}y_2 - y_2\,\mathrm{d}x_2\big)|_{TS^3}. \tag{3}$$

This 1-form is a contact form, in the sense that $\alpha_{\mathrm{st}} \wedge \mathrm{d}\alpha_{\mathrm{st}}$ is a volume form; α_{st} is called the standard contact form on S^3. The Reeb vector field R_{st} of this contact form is defined by $i_{R_{\mathrm{st}}}\mathrm{d}\alpha_{\mathrm{st}} = 0$ and $\alpha_{\mathrm{st}}(R_{\mathrm{st}}) = 1$. Here this means that

$$R_{\mathrm{st}} = x_1\partial_{y_1} - y_1\partial_{x_1} + x_2\partial_{y_2} - y_2\partial_{x_2},$$

which is the vector field giving rise to the Hopf flow.

From this interpretation of the Hopf flow as a Reeb flow, and the contact condition $\alpha_{\mathrm{st}} \wedge \mathrm{d}\alpha_{\mathrm{st}} \neq 0$, we see that the 2-form $\mathrm{d}\alpha_{\mathrm{st}}$ defines an exact area form transverse to the flow of R_{st}, so any surface of section must have non-empty boundary.

For more on the basic notions of contact geometry see [4].

2.1 *d*-Sections

Let $\Sigma \subset S^3$ be a surface of section for the Hopf flow. Then $\partial\Sigma$ is a collection of fibres of the Hopf fibration $S^3 \to S^2$ over a finite number of points $p_1, \ldots, p_k \in S^2$. The interior of Σ projects surjectively to the connected set $S^2 \backslash \{p_1, \ldots, p_k\}$. It follows that each fibre over this set intersects $\mathrm{Int}(\Sigma)$ in the same number of points, and Σ is a d-section for some $d \in \mathbb{N}$, in the following sense.

Definition 2.1 We call an embedded surface $\Sigma \subset S^3$ a *d-section* for the flow of R_{st} if every simple orbit of R_{st} (i.e. every Hopf fibre) intersects $\mathrm{Int}(\Sigma)$ in exactly d points or is a component of $\partial\Sigma$; the latter will be referred to as *boundary fibres*. We shall always orient Σ such that the R_{st}-flow intersects Σ positively. The d-section is said to be *positive* if the boundary orientation of $\partial\Sigma$ coincides with the R_{st}-direction.

In some examples we shall construct such d-sections by starting from an honest multi-section of the Hopf fibration over S^2 with a certain number of discs removed, and then extending it to become tangent to the fibres over the centres of these discs, by gluing in helicoidal surfaces.

2.2 Examples of *d*-Sections

We think of S^3 as being obtained by gluing two copies V_1, V_2 of the solid torus $S^1 \times D^2$. Write μ_i for the meridian and $\lambda_i = S^1 \times \{*\}$, with $* \in \partial D^2$, for the standard longitude on ∂V_i. We shall use those same symbols for any curve on ∂V_i in the same isotopy class. The gluing described by $\mu_1 = \lambda_2$, $\lambda_1 = \mu_2$ yields S^3.

More intrinsically, if one thinks of S^3 as the unit sphere in $\mathbb{C}^2$, we can define V_i as the solid torus given by $\{|z_i| \leq \sqrt{2}/2\}$. The identification of V_1 with $S^1 \times D^2$ is given by

$$V_1 = \left\{ \left(z, \sqrt{1-|z|^2}\, \mathrm{e}^{\mathrm{i}\theta}\right) \colon\ |z| \leq \sqrt{2}/2,\ \theta \in \mathbb{R}/2\pi\mathbb{Z} \right\}.$$

The soul of V_1 is

$$C_1 = \left\{ (0, \mathrm{e}^{\mathrm{i}\theta}) \colon\ \theta \in \mathbb{R}/2\pi\mathbb{Z} \right\},$$

corresponding to $S^1 \times \{0\} \subset S^1 \times D^2$. The solid torus V_2 and its soul C_2 are defined analogously. The μ_i and λ_i are

$$\mu_1 = \left\{ \left(\frac{\sqrt{2}}{2} \mathrm{e}^{\mathrm{i}\theta}, \frac{\sqrt{2}}{2} \right) \colon\ \theta \in \mathbb{R}/2\pi\mathbb{Z} \right\} = \lambda_2$$

and

$$\lambda_1 = \left\{ \left(\frac{\sqrt{2}}{2}, \frac{\sqrt{2}}{2} \mathrm{e}^{\mathrm{i}\theta} \right) \colon\ \theta \in \mathbb{R}/2\pi\mathbb{Z} \right\} = \mu_2.$$

Fig. 1 A helicoidal annulus

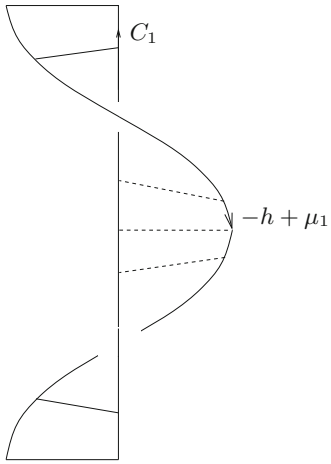

The two souls C_1, C_2 form a positive Hopf link, i.e. the two unknots have linking number $+1$. The *Hopf tori*

$$T_r^2 = \left\{(z_1, z_2) \in S^3 \colon\ |z_1| = r\right\}, \quad r \in]0, 1[,$$

foliate the complement of C_1, C_2 in S^3.

In these coordinates, the Hopf flow is simply the flow of $\partial_{\varphi_1} + \partial_{\varphi_2}$, where φ_i is the angular coordinate in the z_i-plane. The Hopf fibration is then made up of the souls $C_i = S^1 \times \{0\}$ of the two solid tori and the $(1, 1)$-curves on the Hopf tori, i.e. curves in the class $h := \mu_1 + \lambda_1 = \mu_2 + \lambda_2$.

2.2.1 A Disc-Like 1-Section

The disc

$$\left\{\left(\sqrt{1-r^2}, r\mathrm{e}^{\mathrm{i}\theta}\right) \colon\ r \in [0, 1],\ \theta \in \mathbb{R}/2\pi\mathbb{Z}\right\} \subset S^3$$

bounded by C_1 is a positive 1-section for the Hopf flow.

Alternatively, we may identify V_1, V_2 with solid tori such that the Hopf fibres correspond to the S^1-fibres in $S^1 \times D^2$, so that the fibre class is now represented by $h = S^1 \times \{*\}$; this change in identification amounts to a Dehn twist of the solid torus along a meridional disc.

The meridional disc in V_2 defines a 1-section for the Hopf flow in that solid torus. The boundary μ_2 of this disc is identified with $\lambda_1 = h - \mu_1$ in ∂V_1. In V_1 we have a helicoidal surface A with oriented boundary $C_1 \sqcup -(h - \mu_1)$, see Fig. 1. This annulus A glues with the meridional disc in V_2 to form a positive 1-section for the Hopf flow.

2.2.2 An Annular 2-Section

In V_1 we find a helicoidal annulus A_1 with boundary $\partial A_1 = C_1 \sqcup -(h - 2\mu_1)$, with $\mathrm{Int}(A_1)$ intersecting each Hopf fibre positively in two points. Likewise, we have such an annulus A_2 in V_2 with $\partial A_2 = C_2 - (h - 2\mu_2)$. Since

$$h - 2\mu_1 = \lambda_1 - \mu_1 = -(\lambda_2 - \mu_2) = -(h - 2\mu_2),$$

A_1 and A_2 glue to form a positive annular 2-section for the Hopf flow.

Remark 2.2 This annular section is of the same kind as the one found by Poincaré for the planar circular restricted 3-body problem.

2.3 The Euler Number

For the existence of positive d-sections, the sign of the Euler number of the Hopf fibration is crucial.

Lemma 2.3 *The Hopf fibration, regarded as an S^1-bundle over S^2, has Euler number $e = -1$.*

Proof We think of V_1 as in Sect. 2.2.1 as a solid torus $S^1 \times D^2$ with the Hopf fibres given by $S^1 \times \{*\}$. The helicoidal surface $A \subset V_1$ described in Sect. 2.2.1 and Fig. 1, together with the meridional disc in V_2, can be turned into a section of the disc bundle associated with the Hopf bundle by scaling in the fibre direction,

$$V_1 = S^1 \times D^2 \supset \mathrm{Int}(A) \ni \big(a(p), p\big) \longmapsto \big(|p| \cdot a(p), p\big) \in D^2 \times D^2,$$

and extending to a section with a single zero at $p = 0$. Since $\partial A \cap \partial V_1 = \mu_1 - h$ makes one negative twist in the fibre direction as we go once along the boundary μ_1 of the base disc (i.e. the second D^2-factor), this rescaled section, seen as a vector field on D^2, has an index -1 singularity, which means that it cuts the zero section in a single negative point. □

2.4 The Hopf Fibration as a Seifert Fibration

In Sects. 2.5 and 3.2 we are going to show how different descriptions of the Hopf fibration as a Seifert fibration give rise to global surfaces of section with different numbers of boundary components. Here we give a bare bones introduction to Seifert invariants. All necessary background on Seifert fibrations can be found in [6, Section 2]; for a comprehensive treatment see [17].

Consider again S^3 as being obtained by gluing two solid tori V_1, V_2. In terms of meridians μ_1, μ_2 and longitudes h (on both solid tori), the identification of ∂V_1 with ∂V_2 is given by $\mu_1 = \lambda_2 = -\mu_2 + h$ and $h = h$. The curve $-\mu_2$ is the *negative* boundary of the section in V_2 given by a meridional disc. Following the standard conventions for Seifert invariants, see [6], the gluing of the neighbourhoods of the

distinguished fibres in a Seifert manifold should indeed be described with respect to the negative boundary of the section away from the distinguished fibres (which, in the general Seifert setting, include all multiple fibres). This means that the described gluing corresponds to writing S^3 as the Seifert manifold $S^3 = M(0; (1, 1))$. Here 0 is the genus of the base S^2, and $(1, 1)$ are the coefficients of $-\mu_2$ and h in the expression for μ_1.

For a Seifert manifold $M\big(g; (\alpha_1, \beta_1), \ldots, (\alpha_k, \beta_k)\big)$, the Euler number is defined as $-\sum_i \beta_i/\alpha_i$, see [17]. This is consistent with our calculation of the Euler number of the Hopf fibration.

Given such a Seifert manifold $M\big(g; (\alpha_1, \beta_1), \ldots, (\alpha_k, \beta_k)\big)$, one can obtain equivalent descriptions by adding or deleting any pair $(\alpha, \beta) = (1, 0)$, or by replacing each (α_i, β_i) by $(\alpha_i, \beta_i + n_i\alpha_i)$, where $\sum_i n_i = 0$. For instance, the Hopf fibration can alternatively be described as

$$M\big(0; (1, 1), (1, 1), (1, -1)\big), \tag{4}$$

by first adding two pairs $(1, 0)$, and then replacing them by $(1, 1)$ and $(1, -1)$.

2.5 A Pair of Pants 1-Section

We now want to show that the description (4) of the Hopf fibration as a Seifert fibration with three distinguished fibres (albeit of multiplicity 1) gives rise to a pair of pants 1-section with one negative and two positive boundary components, i.e. one component where the boundary orientation is the opposite of the direction of the Hopf flow, and two components where the orientations coincide. An alternative construction illustrates the equivalences between Seifert invariants in terms of a modification of the surface of section. We also describe a third construction that we shall take up again in Sect. 3.4.2.

(i) The description (4) means that we start with a 2-sphere with three open discs removed, i.e. a pair of pants P. Over P the Hopf bundle is the trivial bundle $S^1 \times P$, and we take a constant section there (which we identify with P). Write the negatively oriented boundary $-\partial P$ of P as

$$-\partial P = \sigma_1 \sqcup \sigma_2 \sqcup \sigma_3.$$

We now glue three solid tori V_1, V_2, V_3 to $S^1 \times P$ with gluing map

$$\mu_i = \sigma_i + \beta_i h, \quad h = h,$$

where $\beta_1 = \beta_2 = 1$ and $\beta_3 = -1$. In V_i we find a helicoidal annulus A_i with oriented boundary $\partial A_i = \beta_i C_i \sqcup \sigma_i$, where C_i is the soul of V_i. These three annuli can be glued to P along the σ_i to yield the desired 1-section.

(ii) Alternatively, we can start with a disc-like positive 1-section Σ for the Hopf flow and modify it as follows. Choose a disc $D_0^2 \subset \mathrm{Int}(\Sigma)$. The Hopf fibres passing through D_0^2 define a trivial bundle $S^1 \times D_0^2 \to D_0^2$. Remove the interior of two disjoint discs D_2^2 and D_3^2 from the interior of D_0^2, leaving us with a product bundle over a pair

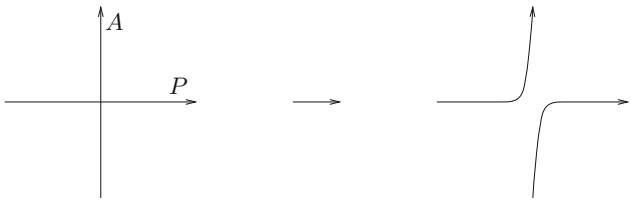

Fig. 2 Gluing A and P

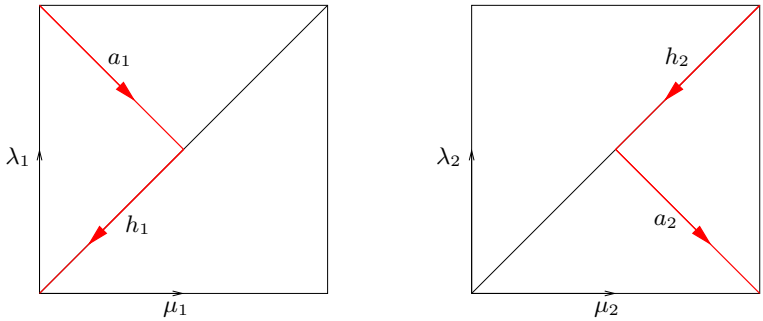

Fig. 3 A pair of pants 1-section

of pants P. In $S^1 \times P$ we find a vertical annulus A with oriented boundary equal to a positive fibre in $S^1 \times \partial D_2^2$ and a negative fibre in $S^1 \times \partial D_3^2$. This annulus can be assumed to intersect the constant section P in a simple curve γ joining ∂D_2^2 with ∂D_3^2.

By slicing open both P and A along γ and regluing them as illustrated (in a cross section) in Fig. 2, one obtains a 1-section with helicoidal boundary curves

$$-\sigma_2 = -\mu_2 + h \quad \text{and} \quad -\sigma_3 = -\mu_3 - h$$

on $S^1 \times \partial D_2^2$ and $S^1 \times \partial D_3^2$, respectively. This 1-section projects diffeomorphically onto P (away from the boundary curves), so it is still a pair of pants.

By gluing in helicoidal annuli A_i in $S^1 \times D_i^2$ with boundary $\partial A_2 = C_2 \sqcup \sigma_2$ and $\partial A_3 = -C_3 \sqcup \sigma_3$, where $C_i = S^1 \times \{0\}$ is the central fibre of $S^1 \times D_i^2$, we obtain again the desired 1-section. This second construction actually explains the equivalences of Seifert invariants that led from the description of the Hopf fibration as $M\big(0; (1, 1)\big)$ to that in (4).

(iii) Here is a third method of construction, which will be useful later on. This time we think of S^3, as at the beginning of Sect. 2.2, as a gluing of two solid tori V_1, V_2 with the identification $\mu_1 = \lambda_2, \lambda_1 = \mu_2$. The Hopf fibration is given by the two souls C_1, C_2 and the $(1, 1)$-curves on the Hopf tori parallel to $\partial V_1 = \partial V_2$.

The simple closed curve $a_1 + h_1$ on ∂V_1, shown in Fig. 3, is homotopic to $-\lambda_1$. This allows us to find an annulus A_1 in V_1 with boundary $\partial A_1 = C_1 \sqcup (a_1 + h_1)$. Likewise, we find an annulus A_2 in V_2 with boundary $\partial A_2 = C_2 \sqcup (h_2 + a_2)$. With the chosen orientations, the A_i intersect each Hopf fibre in $\mathrm{Int}(V_i) \backslash C_i$ once and positively.

Fig. 4 A piecewise linear helix

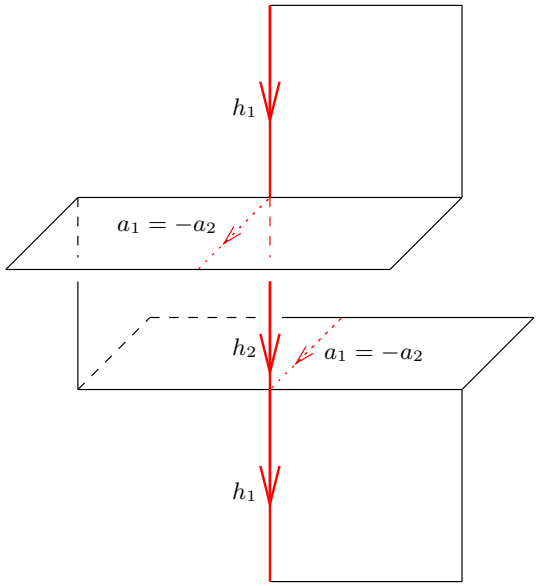

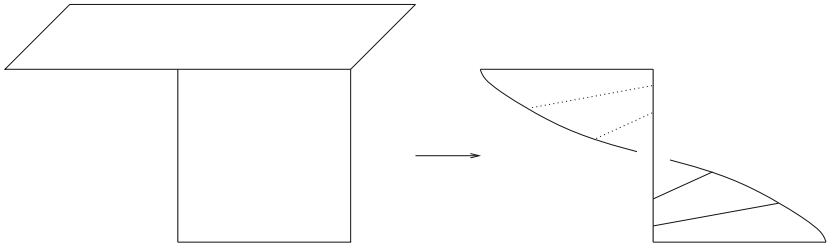

Fig. 5 Smoothening rel boundary fibre

Under the identification of ∂V_1 with ∂V_2, the segment a_1 is mapped to $-a_2$. This allows us to glue A_1 and A_2 along these boundary segments to obtain an oriented pair of pants P with boundary $\partial P = C_1 \sqcup C_2 \sqcup (h_1 + h_2)$. Since $h_1 + h_2$ is a negative Hopf fibre, we have again a 1-section with one negative and two positive boundary components.

Near the boundary component $h_1 + h_2$ in $\partial V_1 = \partial V_2$, this surface P looks as in Fig. 4. This is a piecewise smooth surface that can be smoothened rel boundary fibre into a helicoidal surface, see Fig. 5. From Fig. 4 we also see that this helicoidal surface is a 1-section, for the Hopf fibres near $-(h_1 + h_2)$ are parallel curves with respect to the surface framing given by the 2-torus $\partial V_1 = \partial V_2$. Notice that in Fig. 4 this 2-torus (near the fibre $-(h_1 + h_2)$) is given by the vertical plane determined by that fibre and the line segments $a_1 = -a_2$; the solid torus V_2 sits to the left of this plane, V_1 sits to the right.

3 Lens Spaces

The lens space $L(p, q)$, for $p \in \mathbb{N}$ and q an integer coprime with p, is the oriented three-manifold defined as the quotient of S^3 (with its natural orientation as boundary of the 4-ball in $\mathbb{C}^2$) under the $\mathbb{Z}_p$-action generated by

$$(z_1, z_2) \longmapsto (\mathrm{e}^{2\pi \mathrm{i}/p} z_1, \mathrm{e}^{2\pi \mathrm{i} q/p} z_2).$$

Since this action commutes with the Hopf flow, the flow descends to the quotient. However, the S^1-action on the quotient defined by the Hopf flow will not, in general, be free, so it only defines a Seifert fibration on $L(p, q)$. For a classification of the Seifert fibrations on lens spaces see [6].

3.1 The Lens Spaces $L(d, 1)$

The $\mathbb{Z}_d$-action on S^3 that yields $L(d, 1)$ as the quotient is the one generated by $\Psi_{2\pi/d}$, where Ψ_t is the Hopf flow from (1). Here the $\mathbb{Z}_d$-action is along the Hopf fibres, so the Hopf fibration descends to the quotient to give $L(d, 1)$ the structure of an S^1-bundle over S^2 of Euler number $-d$. This is consistent with the description of $L(d, 1)$ as the manifold obtained from S^3 by surgery along an unknot with framing $-d$, see [7, p. 158].

This S^1-fibration on $L(d, 1)$ corresponds to writing it as the Seifert manifold $L(d, 1) = M\big(0; (1, d)\big)$. Indeed, the gluing $\mu_1 = -\mu_2 + h$, which gave us S^3 in Sect. 2.4, becomes $\mu_1 = -\mu_2 + dh'$ with respect to the shortened fibre h'.

3.2 The Classification of 1-Sections

The S^1-fibration of the lens space $L(d, 1)$, including $S^3 = L(1, 1)$, coming from the Hopf fibration can be written as

$$M\big(0; \underbrace{(1, 1), \ldots, (1, 1)}_{d+k}, \underbrace{(1, -1), \ldots (1, -1)}_{k}\big) \tag{5}$$

with any $k \in \mathbb{N}_0$. This description gives rise to a 1-section with k negative and $d + k$ positive boundaries. Indeed, let Σ_0 be the 2-sphere S^2 with $d+2k$ open discs removed. Write the boundary of Σ_0 with the opposite of its natural orientation as

$$-\partial \Sigma_0 = S^1_0 \sqcup \ldots \sqcup S^1_{d+2k}.$$

The Seifert bundle (5) is then obtained by gluing $d + 2k$ solid tori $V_i = S^1 \times D^2$ to the trivial S^1-bundle $S^1 \times \Sigma_0$ by gluing fibres to fibres (which in the V_i are given by the S^1-factor), and the meridian μ_i of V_i to $S^1_i \pm h$, where h denotes the fibre class, and the sign is positive for $i = 1, \ldots, d + k$, negative for $i = d + k + 1, \ldots, d + 2k$. This means that $S_i = \mu_i \mp h$.

Write $C_i = S^1 \times \{0\}$ for the soul of the solid torus V_i. In V_i we have a helicoidal surface with boundary $\pm C_i \sqcup (\mu_i \mp h)$. These helicoidal surfaces glue with Σ_0 to form a 1-section for the Hopf flow on $L(d, 1)$.

Proposition 3.1 *Any* 1*-section for the Hopf flow on* $L(d, 1)$ *is isotopic to one of those genus* 0 *surfaces just described.*

Proof Let Σ be a 1-section with k_+ positive and k_- negative ends. Remove solid tori V_i around the boundary fibres. In V_i, the 1-section Σ has to look like a helicoidal surface with boundary $\pm C_i \sqcup (\mu_i \mp h)$; this is a consequence of one boundary of $\Sigma \cap V_i$ being $\pm C_i$, and the fact that Σ is a 1-section (cf. Fig. 1).

The part Σ_0 of Σ lying outside the interiors of the V_i defines a trivialisation of the S^1-bundle there, so we can write $L(d, 1) \setminus \cup \operatorname{Int}(V_i)$ as $S^1 \times \Sigma_0$. The identification of the boundary components of Σ_0 (with orientation reversed) with the $\mu_i \mp h$ completely determines the gluing of $S^1 \times \Sigma_0$ with the V_i. Each such gluing contributes ± 1 to the Euler number, so we must have $k_+ = d + k_-$. It follows that Σ is, up to diffeomorphism, one of the surfaces we described above.

Given two such 1-sections with $d + k$ positive and k negative boundaries, we can first isotope them so as to make the boundaries coincide, since any finite set of distinct points on S^2 can be isotoped to any other set of the same cardinality. Near a positive (resp. negative) boundary, the 1-sections look like left-handed (resp. right-handed) helicoidal surfaces making one full turn; any two such surfaces are isotopic.

As before, use one of the two 1-sections to trivialise the complement of open solid tori around the boundary components. In this trivialised complement $S^1 \times \Sigma_0$, the boundary of the other 1-section Σ_0' coincides with that of Σ_0, which implies that Σ_0 and Σ_0' are isotopic rel boundary. □

3.3 *d*-Sections in S^3 Descend to $L(d, 1)$

The following statement will allow us to analyse d-sections for the Hopf flow on S^3 via their induced 1-sections in $L(d, 1)$.

Proposition 3.2 *Any* d*-section for the Hopf flow* Ψ_t *on* S^3 *is isotopic to one that is invariant under the* $\mathbb{Z}_d$*-action generated by* $\Psi_{2\pi/d}$ *and hence descends to a* 1*-section in* $L(d, 1)$.

Proof Near its boundary circles, a d-section looks like a helicoidal surface making d full turns about the central fibre given by the boundary curve. Any such surface is isotopic to a $\mathbb{Z}_d$-invariant helicoid. The remaining part of the d-section is a d-fold covering of a punctured sphere Σ_0, embedded transversely to the fibres in $S^1 \times \Sigma_0$. By isotoping (rel boundary) along the fibres we can ensure that any two adjacent intersections along a fibre occur at a distance $2\pi/d$. □

Corollary 3.3 *Any positive* d*-section for the Hopf flow on* S^3 *is a surface with* d *boundary components.*

Proof By Proposition 3.2, any positive d-section descends to a positive 1-section in $L(d, 1)$. The latter has d boundary components by the classification of 1-sections in Proposition 3.1. □

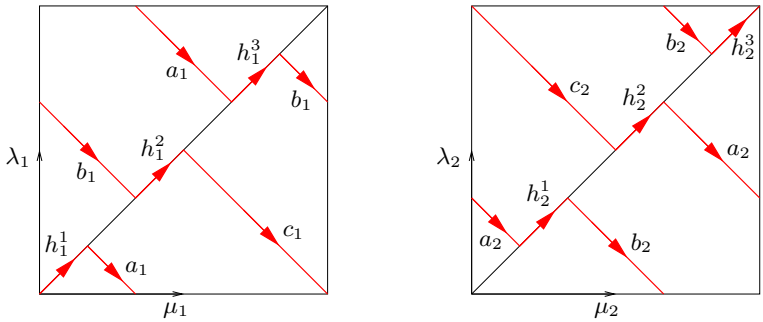

Fig. 6 A positive 3-section of genus 1

3.4 Examples of Invariant *d*-Sections

Before we classify the d-sections for the Hopf fibration, we look at two examples.

3.4.1 A Positive 2-Section

The annular 2-section described in Sect. 2.2.2 is composed of two helicoidal pieces about the boundary fibres C_1 and C_2, glued along their other boundary curves with the identification $h - 2\mu_1 = 2\mu_2 - h$. As we pass to the $\mathbb{Z}_2$-quotient, the two solid tori V_1, V_2 become solid tori with fibre h' of half the length of h. The gluing curves descend to $h' - \mu_1 = \mu_2 - h'$, or $\mu_1 = -\mu_2 + 2h'$. This, as explained in Sect. 2.4, corresponds to the Seifert fibration $M\big(0; (1, 2)\big)$, which is the S^1-bundle over S^2 of Euler class -2, i.e. $L(2, 1)$.

3.4.2 A Positive 3-Section

We now want to exhibit a positive 3-section of genus 1 with three boundary components.

(i) We first use a description as in Sect. 2.5 (iii), see Fig. 6. We think of S^3 as being obtained by gluing two solid tori V_1, V_2 with the identification $\mu_1 = \lambda_2$, $\lambda_1 = \mu_2$. The Hopf fibration is given by the two souls C_1, C_2 and the $(1, 1)$-curves on the Hopf tori.

Write σ_1 for the curve on ∂V_1 made up of the straight line segments h_1^1, a_1, h_1^3, b_1, h_1^2, c_1. Similarly, the curve σ_2 on ∂V_2 is made up of a_2, h_2^1, b_2, h_2^3, c_2, h_2^2. Notice that σ_i is a $(2, -1)$-curve on ∂V_i with respect to the basis (μ_i, λ_i). In V_1 we have a helicoidal annulus A_1 with boundary $\partial A_1 = C_1 \sqcup \sigma_1$; in V_2, an annulus A_2 with $\partial A_2 = C_2 \sqcup \sigma_2$.

Under the identification of ∂V_1 with ∂V_2, the segments a_1, b_1, c_1 are mapped to $-a_2$, $-b_2$, $-c_2$. This allows us to glue A_1 and A_2 along these segments to obtain a surface Σ with boundary consisting of three positive fibres: C_1, C_2 and the one made up of the segments h_i^j. Near this third fibre, Σ can be smoothened as in Fig. 5.

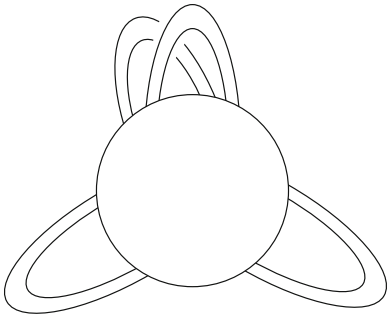

Fig. 7 The topology of the 3-section

The surface Σ is a positive 3-section. Indeed, Σ intersects the Hopf tori in $(2, -1)$-curves; the intersection number of these curves with the Hopf fibres, which are $(1, 1)$-curves, is $(2, -1) \bullet (1, 1) = 3$.

From $2\mu_i - \lambda_i = 3\mu_i - h$ we see that near C_i the surface Σ looks like a left-handed helicoid making three full turns along the fibre, as it should. The same is true for the third component of $\partial\Sigma$, as can bee seen from the explicit gluing construction in Fig. 6 and a comparison with Fig. 4.

The surface Σ is invariant under the $\mathbb{Z}_3$-action generated by $\Psi_{2\pi/3}$, and hence descends to a 1-section in $L(3, 1)$ with three positive boundaries, i.e. a pair of pants.

This 3-section Σ is topologically a surface of genus 1. There are many ways to see this. One is to observe that Σ is obtained by gluing two annuli along three segments in one boundary component of each annulus. This is the same as joining the annuli by one-handles. Joining the two annuli with a single one-handle is the same as attaching two one-handles to a two-disc so as to create a pair of pants. We then attach two further one-handles to the two-disc such that the 'outer' boundary stays connected (since this is the boundary of the helicoidal surface about the fibre made up of the h_i^j) and the surface is orientable. This is a 2-torus with three discs removed, see Fig. 7 or the discussion in [5].

Alternatively, we can appeal to the Riemann–Hurwitz formula. We formulate the relevant result in full generality for positive d-sections.

Proposition 3.4 *Let $\Sigma_{g,d}$ be the connected, closed, orientable surface of genus g with d open discs removed, and S^2_d the 2-sphere with d open discs removed. There is a d-fold unbranched covering $\Sigma_{g,d} \to S^2_d$ if and only if $g = (d-1)(d-2)/2$.*

Proof The 'if' part will follow from the construction of a positive d-section below. For the 'only if' part, we extend the unbranched covering $\Sigma_{g,d} \to S^2_d$ to a branched covering $\Sigma_g \to S^2$ with d branch points upstairs, each of branching index d. Then, by the Riemann–Hurwitz formula, the Euler characteristic of Σ_g is

$$2 - 2g = \chi(\Sigma_g) = d\big(\chi(S^2) - d\big) + d = 3d - d^2,$$

and hence $g = (d-1)(d-2)/2$. □

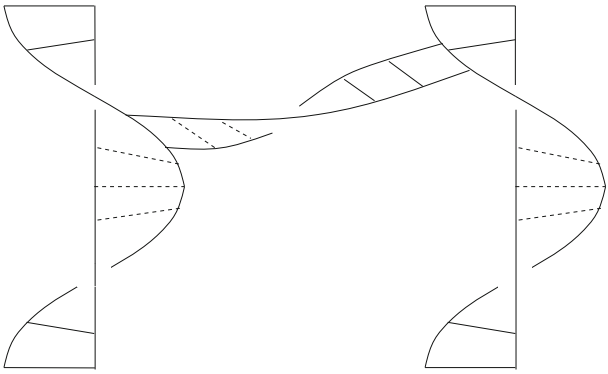

Fig. 8 The 1-section $\overline{\Sigma}$ in $L(3, 1)$ near two boundary fibres

Fig. 9 The projection of $\overline{\Sigma}$ to S^2

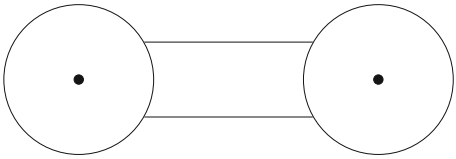

Remark 3.5 In Sect. 4 we give a proof not only of the 'if' part of Proposition 3.4, but also of the 'only if' part, directly from the classification of positive d-sections, which does not use the Riemann–Hurwitz formula.

(ii) Here is an alternative construction of the positive 3-section Σ as a lift of the positive 1-section $\overline{\Sigma}$ in $L(3, 1)$. This construction has the advantage of generalising to all d, while in (i) we made essential use of the fact that there was only one boundary fibre apart from C_1, C_2, which we could place on the Hopf torus $\partial V_1 = \partial V_2$.

Recall from Proposition 3.1 that $\overline{\Sigma}$ is a surface of genus 0 with three boundary components, i.e. a pair of pants. Near any of these boundary components, $\overline{\Sigma}$ looks like a left-handed helicoid making one full turn along the fibre, see Fig. 8.

Consider two of these three helicoids. They project to discs in S^2. Join these discs by a band as shown in Fig. 9. Over this part of S^2 the bundle $L(3, 1) \to S^2$ is trivial, and the two helicoids can be joined by a band to form a 1-section.

The lift of this part of $\overline{\Sigma}$ to S^3 is shown in Fig. 10. Observe that this surface in S^3 has three boundary components: the two special fibres and one further connected component.

If we write μ_0 for the boundary of the disc in S^2 shown in Fig. 7 (oriented positively, i.e. counter-clockwise), and h for the Hopf fibre in S^3, then this third boundary component represents the class $3\mu_0 - 2h$ in the 2-torus in S^3 sitting over μ_0.

Now consider a small disc around the base point in S^2 of the third boundary fibre of $\overline{\Sigma}$. We denote the boundary of this disc by μ_3. Over this disc, $\overline{\Sigma}$ forms a left-handed helicoid making one full turn; its lift Σ to S^3 makes three full turns. Thus, the boundary of this helicoid on the 2-torus in S^3 sitting over μ_3 is the curve $3\mu_3 - h$.

In order to obtain the 3-section Σ in S^3 we need to glue the part shown in Fig. 10 with this third helicoid by identifying $3\mu_0 - 2h$ with $-(3\mu_3 - h)$. This amounts to

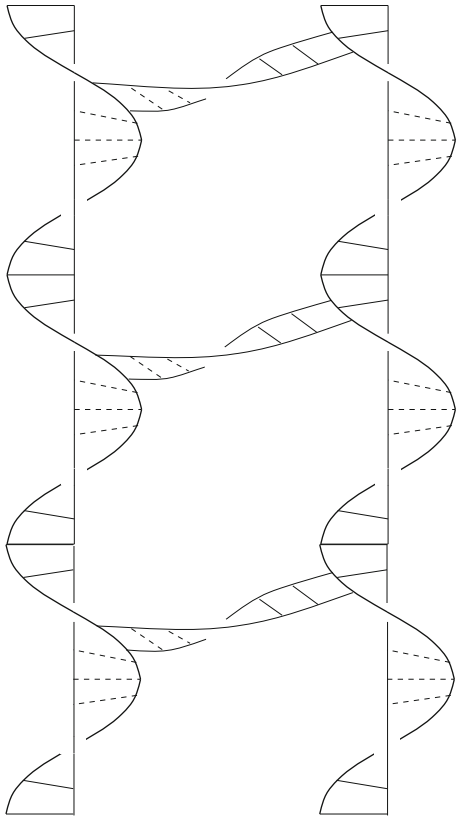

Fig. 10 Alternative view of the positive 3-section

the same as gluing μ_0 with $-\mu_3 + h$, which—as discussed in Sect. 2.4—corresponds to the description of S^3 as $M\big(0; (1, 1)\big)$, so we have indeed found a positive 3-section in S^3.

4 Positive *d*-Sections

We now want to extend the examples from Sect. 3.4 to all natural numbers d, and then give a classification of these d-sections.

4.1 Construction of a Positive *d*-Section

In order to obtain a positive d-section for the Hopf flow, we need to replace the two 3-helicoids in Fig. 10 by $d - 1$ left-handed helicoids making d full twists, joined in sequence by d bands between any two successive helicoids.

First of all, we want to observe that the boundary of this oriented surface consists of one connected component besides the $d - 1$ boundary fibres where the helicoids are attached. Start at a boundary point at the top right of Fig. 10 (generalised to d).

Each time we walk along the boundary of a horizontal band and continue along the boundary of the next helicoid to the left, we move down one level on these helicoids. After having reached the left-most helicoid, we move back to the right along horizontal bands, staying on the same level. When we have returned to the right-most helicoid, we move down one more level until we arrive again at a band going to the left. In the base, this path projects to one full passage along the outer boundary of $\overline{\Sigma}$.

Thus, with each such turn, we have moved down $d-1$ levels. After completing d full turns in the base, the lifted path has covered the whole boundary upstairs. So this boundary upstairs is connected, and it represents the class $d\mu_0-(d-1)h$ on the boundary of the solid torus sitting over $\overline{\Sigma}$. As at the end of the preceding section, we see that this accords with the description of the Hopf fibration as $M\big(0;(1,1)\big)$.

After joining the $d-1$ helicoids in sequence by a single band between any two successive helicoids, we have a surface consisting of $d-1$ one-handles attached to a single two-disc. We then add a further $(d-1)(d-2)$ one-handles, ending up with an oriented surface with d boundary components. Thus, the genus of this surface is

$$g=\frac{1}{2}\big((d-1)^2-(d-1)\big)=\frac{1}{2}(d-1)(d-2).$$

This proves the 'if' part of Proposition 3.4.

4.2 The Classification of Positive *d*-Sections

By considering the choices in the above construction, we arrive at the following classification result. In particular, this reproves the 'only if' part of Proposition 3.4.

Theorem 4.1 *For each $d\in\mathbb{N}$ there is, up to isotopy, a unique positive d-section for the Hopf flow on S^3. It is a connected, orientable surface of genus $(d-1)(d-2)/2$ with d boundary components.*

Proof Let Σ be a positive d-section. Given two distinct points $x,y\in\Sigma$, consider their images $\overline{x},\overline{y}\in S^2$ under the Hopf projection $S^3\to S^2$. Join either of $\overline{x}$ and $\overline{y}$ by a path in S^2 to the base point $\overline{z}$ of a boundary fibre of Σ (such a boundary exists, as observed at the beginning of Sect. 2). These paths lift to paths in Σ joining both x and y with the component of $\partial\Sigma$ over $\overline{z}$. This proves that Σ is connected.

An example of a positive d-section with the claimed topological properties was exhibited above, so it only remains to prove uniqueness up to isotopy. Given two positive d-sections, by Proposition 3.1 we may assume, after an isotopy, that they project to the same 1-section in $L(d,1)$. In particular, the d boundary fibres of the two surfaces sit over the same d points in S^2. Therefore it suffices to show that there are no choices, up to isotopy, in the construction of a positive d-section we described.

The d lifted d-helicoids near the boundary fibres are determined by 1-helicoids of the 1-section in $L(d,1)$. The $d-2$ bands connecting $d-1$ of these helicoids in $L(d,1)$ into a chain lift uniquely to d times $d-2$ bands in S^3 as in Fig. 10: start with a helicoid at the end of the chain and look at the d lifted bands to the neighbouring helicoid. Shifting this helicoid along the fibre by a suitable multiple of $2\pi/d$ will make the bands 'horizontal', so we obtain the standard picture as shown in Fig. 10.

In the remaining construction we join this partial d-section by an annulus with the helicoid around the last boundary fibre. Again, there are no choices up to isotopy. □

5 Complex Projective Curves

In this section we study how algebraic curves $C \subset \mathbb{C}\mathrm{P}^2$ give rise to surfaces of section $\Sigma \subset S^3$ for the Hopf flow. The surface Σ is obtained, under suitable assumptions on C, by radially projecting the affine part $C_{\mathrm{aff}} := C \cap \mathbb{C}^2$ of the algebraic curve, with the origin $(0, 0) \in \mathbb{C}^2$ removed if it happens to lie on C_{aff}, to the unit sphere $S^3 \subset \mathbb{C}^2$.

Intersection points of C with the complex projective line at infinity will correspond to positive boundary components of Σ. If C_{aff} avoids the origin in $\mathbb{C}^2$, there will be no negative boundaries; if $(0, 0) \in C_{\mathrm{aff}}$, this will give rise to negative boundaries.

5.1 Projecting to S^3

For $(a, b) \in S^3 \subset \mathbb{C}^2$, the Hopf circle $\Psi_t(a, b)$, $t \in \mathbb{R}/2\pi\mathbb{Z}$, in S^3 is the image of the punctured radial complex plane

$$P_{a,b} := \left\{(az, bz) \colon\ z \in \mathbb{C}^*\right\}$$

under the radial projection $\mathbb{C}^2 \backslash \{(0, 0)\} \to S^3$. Thus, in order to show that the projection of an algebraic curve $C_{\mathrm{aff}} \subset \mathbb{C}^2 \backslash \{(0, 0)\}$ to S^3 intersects a Hopf circle in d distinct points, we need to show that C_{aff} intersects the corresponding plane $P_{a,b}$ in d distinct points, no two of which lie on the same real ray

$$\left\{r\mathrm{e}^{\mathrm{i}t}(a, b) \colon\ r \in \mathbb{R}^+\right\}.$$

Any complex plane P through the origin in $\mathbb{C}^2$ determines a point P_∞ in the complex projective line $\mathbb{C}\mathrm{P}^1_\infty$ at infinity and vice versa. In order to show that the projection of C_{aff} to S^3 is a positive d-section for the Hopf flow, we need to verify that the projected surface in S^3 becomes asymptotic to the Hopf circles $P \cap S^3$ corresponding to the intersection points $P_\infty \in C \cap \mathbb{C}\mathrm{P}^1_\infty$ (and there should be no intersection points of P with C_{aff} in this case). The positivity of the d-section is ensured by the positivity of complex intersections.

In order to understand the asymptotic behaviour of (not necessarily positive) surfaces of section near their boundary, it will be useful not to look at the projection of $C_{\mathrm{aff}} \backslash \{(0, 0)\}$ to S^3, but rather to regard $C_{\mathrm{aff}} \backslash \{(0, 0)\}$ as a surface in $\mathbb{R} \times S^3$ under the identification of $\mathbb{C}^2 \backslash \{(0, 0)\}$ with the symplectisation $\left(\mathbb{R} \times S^3, \mathrm{d}(\mathrm{e}^{2s}\alpha_{\mathrm{st}})\right)$ of $(S^3, \alpha_{\mathrm{st}})$, with α_{st} as in (3). This identification is given by sending the flow lines of the radial vector field

$$X = \frac{1}{2}(x_1\partial_{x_1} + y_1\partial_{y_1} + x_2\partial_{x_2} + y_2\partial_{y_2})$$

on $\mathbb{C}^2$ to those of $\partial_s/2$. The vector field X is a Liouville vector field for the standard symplectic form $\omega_{\mathrm{st}} = \mathrm{d}x_1 \wedge \mathrm{d}y_1 + \mathrm{d}x_2 \wedge \mathrm{d}y_2$ on $\mathbb{C}^2$, that is, $L_X\omega_{\mathrm{st}} = \omega_{\mathrm{st}}$, and it is homothetic for the standard metric. Therefore, the described identification of $\mathbb{C}^2\backslash\{(0,0)\}$ with $\mathbb{R} \times S^3$ sends the complex structure on $\mathbb{C}^2$ to the standard almost complex structure J on the symplectisation. This J preserves the contact structure $\ker \alpha_{\mathrm{st}}$ and, with R_{st} denoting the Reeb vector field of α_{st}, it satisfies $J\partial_s = R_{\mathrm{st}}$, since $\mathrm{i}X = R_{\mathrm{st}}/2$ along $S^3 \subset \mathbb{C}^2$.

5.2 Homogeneous Affine Polynomials

We begin with the simple situation that the affine curve $C_{\mathrm{aff}} = C \cap \mathbb{C}^2$ is described by a homogeneous polynomial of degree d. We write $[z_0 : z_1 : z_2]$ for the homogeneous coordinates on $\mathbb{C}\mathrm{P}^2$.

Proposition 5.1 *The complex projective curve $C = \{F = 0\} \subset \mathbb{C}\mathrm{P}^2$, where F is a complex polynomial of the form*

$$F(z_0, z_1, z_2) = f(z_1, z_2) - z_0^d,$$

with $f \neq 0$ a homogeneous polynomial of degree d, defines a positive d-section for the Hopf flow on S^3 if and only if F is non-singular.

Proof We first determine the intersection points of the affine part

$$C_{\mathrm{aff}} = \left\{(z_1, z_2) \in \mathbb{C}^2 \colon\ f(z_1, z_2) = 1\right\}$$

(which does not contain the origin $(0,0) \in \mathbb{C}^2$) with the radial planes $P_{a,b}$ in $\mathbb{C}^2$. These intersection points are given by the equation

$$f(a,b)z^d = 1.$$

If $f(a,b) \neq 0$, this equation has d solutions z, related by multiplication by a power of the dth root of unity. Otherwise, there are no solutions.

The partial derivatives of F are given by

$$\frac{\partial F}{\partial z_0} = -dz_0^{d-1}, \quad \frac{\partial F}{\partial z_1} = \frac{\partial f}{\partial z_1}, \quad \text{and} \quad \frac{\partial F}{\partial z_2} = \frac{\partial f}{\partial z_2}.$$

For $z_0 \neq 0$ we have $\partial F/\partial z_0 \neq 0$, so the affine part is always non-singular.

We now look at the points of C in

$$\mathbb{C}\mathrm{P}^1_\infty = \left\{[z_0 : z_1 : z_2] \in \mathbb{C}\mathrm{P}^2 \colon\ z_0 = 0\right\}.$$

Solutions of $F = 0$ of the form $[0 : a : b]$ are determined by the equation $f(a,b) = 0$. In other words, a point at infinity lies on C precisely when C does *not* intersect the radial plane in $\mathbb{C}^2$ determined by that point.

Now, the projection of C_{aff} to S^3 extends to a positive d-section precisely when it is asymptotic to d distinct Hopf orbits. This amounts to saying that the equation $f(a, b) = 0$ should have d distinct solutions $[a : b] \in \mathbb{C}\mathrm{P}^1$, which is equivalent to f being non-singular. This, in turn, is equivalent to F being non-singular.

It remains to check that C_{aff} has the correct asymptotic behaviour near these d Hopf orbits. Let $[a_1 : b_1] \in \mathbb{C}\mathrm{P}^1$ be a solution of $f(a, b) = 0$. We may assume without loss of generality that $a_1 \neq 0$. For a small $\varepsilon > 0$ the curve

$$\theta \longmapsto [a_\theta : b_\theta] := [a_1 : b_1 + \varepsilon a_1 \mathrm{e}^{\mathrm{i}\theta}], \quad \theta \in S^1 = \mathbb{R}/2\pi\mathbb{Z},$$

describes a circle in $\mathbb{C}\mathrm{P}^1$ around the point $[a_1 : b_1]$.

The points of C_{aff} (projected to S^3) in the Hopf fibre over $[a_\theta : b_\theta]$ are given by the solutions w_θ of the equation $f(a_\theta, b_\theta) w_\theta^d = 1$, and then radially projecting the points $(a_\theta w_\theta, b_\theta w_\theta)$ to S^3. As θ makes one full turn in S^1, the function $\arg\big(f(a_\theta, b_\theta)\big)$ likewise makes one complete turn, provided $\varepsilon > 0$ is sufficiently small. This can be seen by factorising f as

$$f(z_1, z_2) = (b_1 z_1 - a_1 z_2) \cdots (b_d z_1 - a_d z_2)$$

with the a_j, b_j describing d distinct points $[a_j : b_j] \in \mathbb{C}\mathrm{P}^1$.

Thus, if we choose a solution w_0 and then define w_θ, $\theta \in \mathbb{R}$, continuously in θ, we have $w_{\theta+2\pi} = \mathrm{e}^{-2\pi\mathrm{i}/d} w_\theta$. This guarantees that the projection of C_{aff} to S^3 does indeed look like a left-handed d-fold helicoid about a Hopf fibre near each of its d boundary components. □

In particular, for $d = 1$ the polynomial F describes a projective line $L \neq \mathbb{C}\mathrm{P}^1_\infty$, since $f \neq 0$. This line has a single point at infinity, and the projection of the affine part $L_{\mathrm{a}} = L \cap \mathbb{C}^2$ to S^3 defines a disc-like 1-section for the Hopf flow.

Remark 5.2 For the final part of the proof of Proposition 5.1, the asymptotic behaviour near the boundary components, one may also look at the behaviour of C_{aff} near $s = \infty$ under the identification of $\mathbb{C}^2 \backslash \{(0, 0)\}$ with $\mathbb{R} \times S^3$ described in Sect. 5.1. The tangent spaces of C_{aff} contain vectors getting closer and closer to ∂_s as we approach $s = \infty$, and hence also tangent vectors close to the Reeb vector field $R_{\text{st}} = J\partial_s$. This suffices to see that C_{aff} becomes asymptotic to a Reeb orbit, but it does not guarantee, as our *ad hoc* argument does, that this orbit will only be simply covered.

5.3 Algebraic Curves Giving Rise to 1-Sections

We next want to describe a class of homogeneous polynomials $F(z_0, z_1, z_2)$ of degree d that give rise to 1-sections for the Hopf flow with d positive and $d - 1$ negative boundary components.

Write $f_k(z_1, z_2)$ for a non-zero homogeneous polynomial of degree k. As in the previous section, we can factorise this as

$$f_k(z_1, z_2) = c_k (b_1^k z_1 - a_1^k z_2) \cdots (b_k^k z_1 - a_k^k z_2)$$

with $c_k \in \mathbb{R}^+$ and $(a_j^k, b_j^k) \neq (0,0)$. The factor c_k in this expression allows us to assume without loss of generality that the (a_j^k, b_j^k) lie in $S^3 \subset \mathbb{C}^2$.

The following is easy to see.

Lemma 5.3 *Let $C = \{F = 0\} \subset \mathbb{C}\mathrm{P}^2$ be the algebraic curve defined by*

$$F(z_0, z_1, z_2) = f_d(z_1, z_2).$$

With notation as above, we assume that the $[a_j^d : b_j^d] \in \mathbb{C}\mathrm{P}^1$ are pairwise distinct for $j = 1, \ldots, d$. Then $C_{\mathrm{aff}} \backslash \{(0,0)\} \subset \mathbb{R} \times S^3$ defines a collection of d cylinders $\mathbb{R} \times \gamma$ over the Hopf fibres γ through the points $(a_j^d, b_j^d) \in S^3$. □

Next we look at polynomials defined by a pair f_d, f_{d-1}.

Proposition 5.4 *Let F be a homogeneous complex polynomial of degree d of the form*

$$F(z_0, z_1, z_2) = f_d(z_1, z_2) + z_0 f_{d-1}(z_1, z_2),$$

and $C = \{F = 0\} \subset \mathbb{C}\mathrm{P}^2$. With notation as above, we assume that the $[a_j^k : b_j^k] \in \mathbb{C}\mathrm{P}^1$ are pairwise distinct for $k \in \{d-1, d\}$ and $1 \leq j \leq k$. Then the projection of $C_{\mathrm{aff}} \backslash \{(0,0)\}$ to S^3 defines a 1-section for the Hopf flow with d positive and $d-1$ negative boundary components, given by the Hopf fibres through the points (a_j^d, b_j^d) and (a_j^{d-1}, b_j^{d-1}), respectively.

Proof Observe that C is non-singular, since a common zero $[z_0 : z_1 : z_2]$ of F and $\partial F / \partial z_0 = f_{d-1}$ would also have to be a zero of f_d, which our assumptions rule out.

The case $d = 1$ is covered by Proposition 5.1, so we assume $d \geq 2$ from now on.

There are d distinct points at infinity on the curve C, as $C \cap \mathbb{C}\mathrm{P}^1_\infty$ is given by the equation $f_d = 0$. The intersection of C_{aff} with a (punctured) radial plane $P_{a,b}$ is described by the equation

$$f_d(a,b)z + f_{d-1}(a,b) = 0, \quad z \neq 0.$$

There are no solutions if $f_d(a,b) = 0$, since this would force a common zero with f_{d-1}. Likewise, there is no solution if $f_{d-1}(a,b) = 0$. For $f_d(a,b)$, $f_{d-1}(a,b) \neq 0$, there is a unique intersection point of C_{aff} with $P_{a,b}$. This proves that $C_{\mathrm{aff}} \backslash \{(0,0)\}$ projects to a 1-section for the Hopf flow away from the Hopf fibres over the points $[a_j^k : b_j^k]$.

For the asymptotic behaviour near these fibres, we consider a small circle $\theta \mapsto [a_\theta : b_\theta] \in \mathbb{C}\mathrm{P}^1$ around a solution $[a : b]$ of $f_d = 0$ or $f_{d-1} = 0$, as in the proof of Proposition 5.1. The point of the 1-section in the Hopf fibre over $[a_\theta : b_\theta]$ is given by radially projecting the point $(a_\theta w_\theta, b_\theta w_\theta)$ to S^3, with w_θ determined by

$$w_\theta = -\frac{f_{d-1}(a_\theta, b_\theta)}{f_d(a_\theta, b_\theta)}.$$

As we encircle a zero of f_d, the argument of w_θ makes one negative rotation; around a zero of f_{d-1}, a positive one. Thus, near these fibres the 1-section looks like a left-handed resp. right-handed helicoid. □

Remark 5.5

(1) By Proposition 3.1, the 1-sections found in Proposition 5.4 are of genus 0.
(2) For the asymptotic behaviour of $C_{\text{aff}}\backslash\{(0,0)\} \subset R \times S^3$ near $s = -\infty$ we may alternatively observe that as $C_{\text{aff}} \ni (z_1, z_2) \to (0,0)$, the surface becomes asymptotic to the surface given by $f_{d-1} = 0$, which by Lemma 5.3 is a cylinder over a Hopf fibre. The same caveat as in Remark 5.2 applies.

6 Holomorphic Buildings and the Degree–Genus Formula

In this section we present two proofs of the degree-genus formula.

Theorem 6.1 *Any non-singular algebraic curve $C \subset \mathbb{C}\mathrm{P}^2$ of degree d is homeomorphic to a closed, connected orientable surface of genus $g = (d-1)(d-2)/2$.*

One proof only uses the classification of d-sections for the Hopf flow. The second proof uses degenerations of complex algebraic curves into holomorphic buildings in the sense of symplectic field theory. This second proof yields an explanation of the degree-genus formula as a sum $\sum_{k=1}^{d-2} k$. Either proof relies on the fact that, as a consequence of Bertini's theorem [9, Lecture 17], the general (in the sense of [9, p. 53]) algebraic curve of degree d in $\mathbb{C}\mathrm{P}^2$ is non-singular.

The projective space of homogeneous polynomials $F(z_0, z_1, z_2)$ of degree d is of dimension $N = (d^2 + 3d)/2$, since there are $(d+2)(d+1)/2$ monomials of degree d in three variables. There is an embedding $\mathbb{C}\mathrm{P}^2 \to \mathbb{C}\mathrm{P}^N$ given by sending the point $[z_0 : z_1 : z_2]$ to $[\ldots : z^I : \ldots]$, where z^I ranges over all monomials of degree d in three variables. The image of this embedding is the Veronese variety [9, p. 23], which is a smooth variety.

The algebraic curves of degree d in $\mathbb{C}\mathrm{P}^2$ are exactly the hyperplane sections of the Veronese variety. To this description of algebraic curves one can apply Bertini's theorem on the smoothness of hyperplane sections to conclude that the subset of non-singular algebraic curves in the space of all algebraic curves of degree d is open, dense, and connected. Under deformations through non-singular curves, the topological genus is invariant.

A slightly more direct (and more sophisticated) argument can be based on the version of Bertini's theorem proved in [10, Corollary III.10.9]. The projective space of degree d homogeneous polynomials in three variables (or the set of divisors made up of the curves defined by these polynomials) is a linear system (see also [8, Section 1.1] for a discussion of linear systems more accessible to non-algebraic geometers). This linear system is without base points, i.e. for every point in $\mathbb{C}\mathrm{P}^2$ there is an algebraic curve of degree d *not* containing the given point. Then Bertini's theorem says that almost every element of this linear system, that is, every element outside a lower-dimensional subvariety, is non-singular.

First proof of Theorem 6.1 The algebraic curves C of degree d in Proposition 5.1 have d distinct points at infinity, and their affine part C_{aff} does not contain the origin. The projection of C_{aff} to S^3 defines a positive d-section. By Theorem 4.1 this means that, when viewed in $\mathbb{R} \times S^3$, the complex curve C_{aff} is topologically a connected, orientable surface of genus $g = (d-1)(d-2)/2$ with d ends asymptotic to cylinders over Hopf fibres. The algebraic curve C is obtained topologically by capping off these ends with discs.

This proves the degree-genus formula for the algebraic curves described in Proposition 5.1. For the general case, it suffices to appeal to the connectedness of the space of non-singular curves of degree d. □

Our second proof illustrates the degeneration phenomena in symplectic field theory.

Second proof of Theorem 6.1 After a projective transformation of $\mathbb{C}\mathrm{P}^2$ we may assume that $[1:0:0] \notin C$. Then C can be written as $\{F = 0\}$ with F of the form

$$F(z_0, z_1, z_2) = f_d(z_1, z_2) + z_0 f_{d-1}(z_1, z_2) + \cdots + z_0^{d-1} f_1(z_1, z_2) + z_0^d.$$

By a small perturbation of F we may assume that each f_k has k distinct zeros, and no adjacent pair f_k, f_{k-1} has zeros in common. In particular, the intersection $C \cap \mathbb{C}\mathrm{P}^1_\infty$ then consists of d non-singular points, and we shall focus our attention on the affine part C_{aff}. As before, topologically the closed surface C is obtained by capping off the d ends of C_{aff} with discs. Since the subspace of singular curves is of real codimension 2 by Bertini's theorem, we may further assume that the whole family

$$\begin{aligned} f^\lambda(z_1, z_2) := {} & f_d(z_1, z_2) + \lambda f_{d-1}(z_1, z_2) + \lambda^3 f_{d-2}(z_1, z_2) + \cdots \\ & \cdots + \lambda^{d(d-1)/2} f_1(z_1, z_2) + \lambda^{(d+1)d/2}, \quad \lambda \in (0, 1], \end{aligned}$$

where the power of λ multiplying f_{d-k} is $\sum_{j=0}^{k} j$, consists of non-singular polynomials. Notice that none of these curves $C^\lambda = \{f^\lambda = 0\}$ contains the origin in $\mathbb{C}^2$, so we may think of this as a family of curves $C^\lambda \subset \mathbb{R} \times S^3$.

Our aim is to determine the topological genus of the affine curve $\{f^1 = 0\}$, which is a curve with d boundary components. In the naive limit $\lambda \to 0$ we lose all topological information, since by Lemma 5.3 the curve $\{f_d = 0\} \backslash \{(0, 0)\}$ is simply a collection of d cylinders, for as $\lambda \to 0$, the topology of C^λ disappears towards $-\infty$ in $\mathbb{R} \times S^3$.

In the spirit of SFT [3], we now rescale the curve in different ways during this limit process $\lambda \to 0$, which amounts to zooming in at different parts of the curve to see its topology. We first present the heuristic argument; details of the convergence process will be discussed in Sect. 7.

For the rescaling, we replace (z_1, z_2) by $c_\lambda(z_1, z_2)$, with judicious choices of the scaling factor c_λ. The rescaling leads to the family of polynomials

$$f_*^\lambda = c_\lambda^d f_d + \lambda c_\lambda^{d-1} f_{d-1} + \lambda^3 c_\lambda^{d-2} f_{d-2} + \cdots + \lambda^{d(d-1)/2} c_\lambda f_1 + \lambda^{(d+1)d/2}.$$

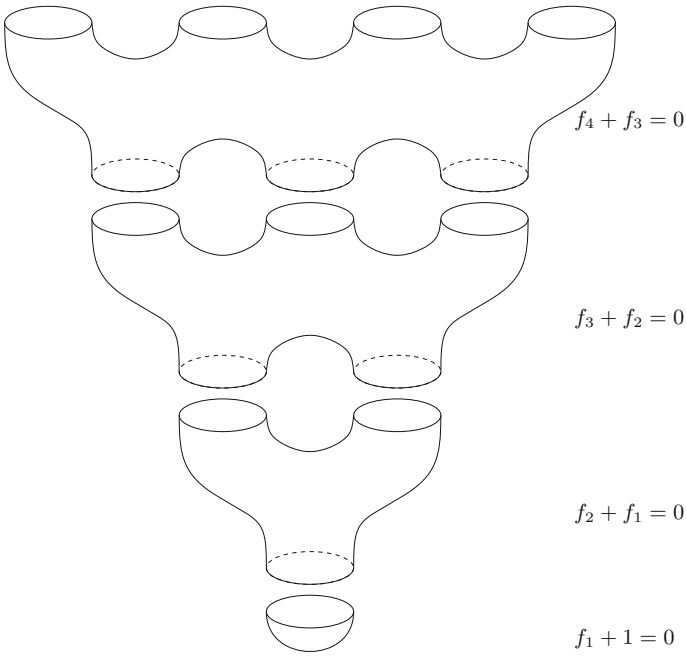

Fig. 11 A holomorphic building from a degree 4 curve

We now choose $c_\lambda = \lambda^k$ for some $1 \leq k \leq d$. Then the polynomials f_{d-k+1} and f_{d-k} are multiplied by the same power

$$k(d-k+1) + \sum_{j=0}^{k-1} j = k(d-k) + \sum_{j=0}^{k} j$$

of λ, whereas all other summands contain a larger power of λ. Hence, as $\lambda \to 0$ the rescaled polynomial

$$f_*^\lambda / \lambda^{k(d-k)+\sum_{j=0}^{k} j}$$

converges to $f_{d-k+1} + f_{d-k}$, which for $k = d$ has to be read as $f_1 + 1$. By Remark 5.5 (1), this defines a surface of genus 0 with $d-k+1$ positive and $d-k$ negative boundaries at $\pm\infty$, respectively, in $\mathbb{R} \times S^3$.

As shown in Proposition 5.4, the curve $\{f_{d-k+1} + f_{d-k} = 0\} \backslash \{(0,0)\}$ is asymptotic to the Hopf fibres determined by the zeros of f_{d-k+1} and f_{d-k} at $+\infty$ and $-\infty$, respectively. Hence, these limits for the different choices of rescaling c_λ fit together into a holomorphic building in the sense of SFT as shown in Fig. 11.

Observe that intermediate rescalings only lead to trivial cylinders over the boundary orbits and hence do not carry any additional topology. For instance, if we choose

$c_\lambda = \lambda^{3/2}$, then

$$f_*^\lambda = \lambda^{3d/2} f_d + \lambda^{(3d-1)/2} f_{d-1} + \lambda^{3d/2} f_{d-2} + \cdots,$$

and after rescaling only the polynomial f_{d-1} will survive in the limit. Then refer to Lemma 5.3.

Thus, the genus of C can be read off the holomorphic building we obtain in this SFT limit. The individual levels carry no genus, and the gluing of two adjacent levels adds #(limit orbits) $-$ 1 to the genus. We conclude that the genus of the curve C of degree d is given by $\sum_{k=1}^{d-2} k = (d-1)(d-2)/2$. □

Example 6.2 Here is a concrete example that illustrates the essential aspects in the following discussion of convergence. Suppose we would like to understand the topology of the Fermat curve of degree 3,

$$\left\{[z_0 : z_1 : z_2] \in \mathbb{C}\mathrm{P}^2 \colon\ z_0^3 + z_1^3 + z_2^3 = 0\right\}.$$

We consider the affine part

$$\left\{(z_1, z_2) \in \mathbb{C}^2 \colon\ z_1^3 + z_2^3 + 1 = 0\right\}.$$

We now introduce terms of lower order and a family parameter λ:

$$f^\lambda(z_1, z_2) = z_1^3 + z_2^3 + \lambda(z_1^2 + z_2^2) + \lambda^3(z_1 + z_2) + \lambda^6.$$

When we evaluate f^λ at $(\lambda z_1, \lambda z_2)$, we obtain

$$f^\lambda(\lambda z_1, \lambda z_2) = \lambda^3(z_1^3 + z_2^3 + z_1^2 + z_2^2) + \lambda^4(z_1 + z_2) + \lambda^6;$$

rescaling with λ^2 yields

$$f^\lambda(\lambda^2 z_1, \lambda^2 z_2) = \lambda^6(z_1^3 + z_2^3) + \lambda^5(z_1^2 + z_2^2 + z_1 + z_2) + \lambda^6;$$

the third rescaling to consider is

$$f^\lambda(\lambda^3 z_1, \lambda^3 z_2) = \lambda^9(z_1^3 + z_2^3) + \lambda^7(z_1^2 + z_2^2) + \lambda^6(z_1 + z_2 + 1).$$

After dividing these polynomials by λ^3, λ^5 and λ^6, respectively, we see that in the limit $\lambda \to 0$ we obtain the respective polynomials

$$z_1^3 + z_2^3 + z_1^2 + z_2^2, \quad z_1^2 + z_2^2 + z_1 + z_2, \quad z_1 + z_2 + 1.$$

7 SFT Convergence

In this section we fill in the technical details of the second proof of Theorem 6.1.

7.1 Convergence of Submanifolds

In order to understand the convergence of submanifolds defined by equations, we consider the following general situation. Let $M \subset \mathbb{R}^n$ be a compact submanifold of codimension k defined globally by k smooth functions $h_1, \ldots, h_k \colon \mathbb{R}^n \to \mathbb{R}$. This means that

$$M = \{h_1 = \ldots = h_k = 0\},$$

with the gradient vector fields $\nabla h_1, \ldots, \nabla h_k$ pointwise linearly independent along the common zero set M of the h_i. In particular, the normal bundle of M is trivial, and we find a tubular neighbourhood νM of $M \subset \mathbb{R}^n$ diffeomorphic to $M \times D^k$ such that at each point of $M \times D^k$ the orthogonal complement to the span of $\nabla h_1, \ldots, \nabla h_k$ is transverse to the D^k-factor.

We may assume that there is an $\varepsilon > 0$ such that at any point outside the tubular neighbourhood νM, at least one of the functions $|h_i|$ takes a value larger than ε. Now let $d_1, \ldots, d_k \colon \mathbb{R}^n \to [-1, 1]$ be smooth functions. Then, for $|\lambda| < \varepsilon$, the common zero set of the functions $h_i + \lambda d_i$ lies inside νM. By shrinking νM and ε we can ensure that the gradient vector fields $\nabla h_i + \lambda \nabla d_i$ are pointwise linearly independent on νM for any $|\lambda| < \varepsilon$, and the orthogonal complement to their span is transverse to the D^k-factor.

Under these assumptions, the common zero set

$$M_\lambda = \{h_1 + \lambda d_1 = \ldots = h_k + \lambda d_k = 0\}$$

will be a submanifold contained in $\nu M = M \times D^k$ for $|\lambda| < \varepsilon$, given as the graph of a map $M \to D^k$. In particular, M_λ will be an isotopic copy of M.

7.2 Degeneration of Algebraic Curves

We now return to the specific situation of Sect. 6. We write $(z_1, z_2) = \mathrm{e}^t q$ with $t \in \mathbb{R}$ and $q \in S^3 \subset \mathbb{C}^2$. Set

$$g_k = f_k|_{S^3}, \quad k = 0, \ldots, d,$$

where $f_0 = 1$. Then

$$G^\lambda(t, q) := f^\lambda(\mathrm{e}^t q) = \sum_{\ell=0}^{d} \mathrm{e}^{(d-\ell)t} \lambda^{\ell(\ell+1)/2} g_{d-\ell}(q).$$

The rescaling of (z_1, z_2) by a constant factor amounts to a shift in the t-coordinate, so we set

$$G^\lambda_\mu(t, q) = g^\lambda(t + \mu \log \lambda, q) = \sum_{\ell=0}^{d} \mathrm{e}^{(d-\ell)t} \lambda^{\mu(d-\ell)+\ell(\ell+1)/2} g_{d-\ell}(q).$$

The choice $\mu = k$ corresponds to f_*^λ with $c_\lambda = \lambda^k$ in the second proof of Theorem 6.1.

7.3 Convergence to a Holomorphic Building

With this choice $\mu = k$ we want to get a quantitative understanding of the convergence of the rescaled function

$$\frac{G_k^\lambda(t,q)}{\lambda^{k(d-k)+k(k+1)/2}} = \frac{1}{\lambda^{k(d-k)+k(k+1)/2}} \sum_{\ell=0}^{d} \mathrm{e}^{(d-\ell)t} \lambda^{k(d-\ell)+\ell(\ell+1)/2} g_{d-\ell}(q) \tag{6}$$

to

$$G_k^0(t,q) = \mathrm{e}^{(d-k+1)t} g_{d-k+1}(q) + \mathrm{e}^{(d-k)t} g_{d-k}(q) \tag{7}$$

for $\lambda \to 0$. Notice that the summands in (6) that vanish in the limit are of the form

$$\lambda^m \mathrm{e}^{(d-k+1+n)t} g_{d-k+1+n}(q) \quad \text{or} \quad \lambda^m \mathrm{e}^{(d-k-n)t} g_{d-k-n}(q)$$

with $m \geq n > 0$. On any compact interval $t \in [-N, N]$, these summands go uniformly to zero for $\lambda \to 0$, but we can do a little better than that.

For large positive t, the first summand in (7) dominates, so we consider the rescaled function

$$G_k^+(t,q) = g_{d-k+1}(q) + \mathrm{e}^{-t} g_{d-k}(q); \tag{8}$$

for $t < 0$ with $|t|$ large, we look at

$$G_k^-(t,q) = \mathrm{e}^{t} g_{d-k+1}(q) + g_{d-k}(q).$$

Lemma 7.1 *On* $[0, -\frac{3}{4}\log\lambda] \times S^3$, *the rescaled function*

$$\frac{G_k^\lambda(t,q)}{\lambda^{k(d-k)+k(k+1)/2}\,\mathrm{e}^{(d-k+1)t}}$$

converges uniformly to $G_k^+(t,q)$ *for* $\lambda \to 0$.

On $[\frac{3}{4}\log\lambda, 0] \times S^3$, *the rescaled function*

$$\frac{G_k^\lambda(t,q)}{\lambda^{k(d-k)+k(k+1)/2}\,\mathrm{e}^{(d-k)t}}$$

converges uniformly to $G_k^-(t,q)$ *for* $\lambda \to 0$.

Proof For $t \in [0, -\frac{3}{4}\log\lambda]$ and $m \geq n > 0$ as above, we have

$$\lambda^m \mathrm{e}^{nt} < \lambda^{m-3n/4} \longrightarrow 0$$

for $\lambda \to 0$. The other case is analogous. □

Remark 7.2 Notice that the domain of convergence increases as λ gets smaller. By uniform convergence we mean that for any $\varepsilon > 0$ there is a $\lambda_0 = \lambda_0(\varepsilon)$ such that for any $\lambda < \lambda_0$ the function (8) is ε-close to $G_k^+(t, q)$ for all $(t, q) \in [0, -\frac{3}{4}\log\lambda] \times S^3$, similarly for the other case. This statement remains true for any finite number of derivatives, with a smaller $\lambda_0(\varepsilon)$.

The considerations of Sect. 7.1 now imply that for λ sufficiently close to 0, the curve

$$C^\lambda \cap [k + \frac{3}{4}\log\lambda, k - \frac{3}{4}\log\lambda]$$

has the topology of $\{f_{d-k+1} + f_{d-k} = 0\}$. The intervals $[k + \frac{3}{4}\log\lambda, k - \frac{3}{4}\log\lambda]$ overlap for adjacent k, and similar considerations show that in the region of overlap the topology of C^λ is that of a collection of cylinders over Reeb orbits.

This concludes the convergence argument in the second proof of Theorem 6.1.

Acknowledgements This paper was initiated during an enjoyable stay at Schloß Rauischholzhausen, the conference centre of JLU Gießen. We thank the castle staff for creating an inspiring research environment. We are grateful to Stefan Kebekus for useful correspondence on algebraic curves, and to Jean Gutt for comments on a draft version of this paper.

Funding Open Access funding enabled and organized by Projekt DEAL.

Open Access This article is licensed under a Creative Commons Attribution 4.0 International License, which permits use, sharing, adaptation, distribution and reproduction in any medium or format, as long as you give appropriate credit to the original author(s) and the source, provide a link to the Creative Commons licence, and indicate if changes were made. The images or other third party material in this article are included in the article's Creative Commons licence, unless indicated otherwise in a credit line to the material. If material is not included in the article's Creative Commons licence and your intended use is not permitted by statutory regulation or exceeds the permitted use, you will need to obtain permission directly from the copyright holder. To view a copy of this licence, visit http://creativecommons.org/licenses/by/4.0/.

References

1. Abbondandolo, A., Bramham, B., Hryniewicz, U.L., Salomão, P.A.S.: Sharp systolic inequalities for Reeb flows on the 3-sphere. Invent. Math. **211**, 687–778 (2018)
2. Albers, P., Geiges, H., Zehmisch, K.: Pseudorotations of the 2-disc and Reeb flows on the 3-sphere. Ergodic Theory Dyn. Syst. **(to appear)**
3. Bourgeois, F., Eliashberg, Ya., Hofer, H., Wysocki, K., Zehnder, E.: Compactness results in symplectic field theory. Geom. Topol. **7**, 799–888 (2003)
4. Geiges, H.: An Introduction to Contact Topology, Cambridge Studies in Advanced Mathematics, vol. 109. Cambridge University Press, Cambridge (2008)
5. Geiges, H.: How to depict 5-dimensional manifolds. Jahresber. Dtsch. Math.-Ver. **119**, 221–247 (2017)
6. Geiges, H., Lange, C.: Seifert fibrations of lens spaces. Abh. Math. Sem. Univ. Hambg. **88**, 1–22 (2018)
7. Gompf, R.E., Stipsicz, A.I.: 4-Manifolds and Kirby Calculus, Graduate Studies in Mathematics, vol. 20. American Mathematical Society, Providence (1999)
8. Griffiths, P., Harris, J.: Principles of Algebraic Geometry. Wiley-Interscience, New York (1978)
9. Harris, J.: Algebraic Geometry—A First Course, Graduate Texts in Mathematics, vol. 133. Springer, Berlin (1992)
10. Hartshorne, R.: Algebraic Geometry, Graduate Texts in Mathematics, vol. 52. Springer, Berlin (1977)
11. Hofer, H., Wysocki, K., Zehnder, E.: The dynamics on three-dimensional strictly convex energy surfaces. Ann. Math. (2) **148**, 197–289 (1998)

12. Hofer, H., Wysocki, K., Zehnder, E.: Finite energy foliations of tight three-spheres and Hamiltonian dynamics. Ann. Math. (2) **157**, 125–255 (2003)
13. Hryniewicz, U., Momin, A., Salomão, P.A.S.: A Poincaré-Birkhoff theorem for tight Reeb flows on S^3. Invent. Math. **199**, 333–422 (2015)
14. Hryniewicz, U., Salomão, P.A.S.: On the existence of disk-like global sections for Reeb flows on the tight 3-sphere. Duke Math. J. **160**, 415–465 (2011)
15. Hryniewicz, U.L., Salomão, P.A.S.: Global surfaces of section for Reeb flows in dimension three and beyond. In: Proceedings of the International Congress of Mathematicians (Rio de Janeiro, 2018), vol. 1, pp. 937–964
16. Hutchings, M.: Mean action and the Calabi invariant. J. Mod. Dyn. **10**, 511–539 (2016)
17. Jankins, M., Neumann, W.D.: Lectures on Seifert Manifolds, Brandeis Lecture Notes, vol. 2. Brandeis University, Waltham (1983). http://www.math.columbia.edu/~neumann/preprints/. Accessed 10 Dec 2021
18. Kirwan, F.: Complex Algebraic Curves, London Mathematical Society Student Texts, vol. 23. Cambridge University Press, Cambridge (1992)
19. van Koert, O.: A Reeb flow on the three-sphere without a disk-like global surface of section. Qual. Theory Dyn. Syst. **19**, Art. 36 (2020)
20. Prasolov, V.V., Sossinsky, A.B.: Knots, Links, Braids and 3-Manifolds, Translations of Mathematical Monographs, vol. 154. American Mathematical Society, Providence (1997)

Publisher's Note Springer Nature remains neutral with regard to jurisdictional claims in published maps and institutional affiliations.